Pu and Lin *Geosci. Lett.* (2015) 2:11
DOI 10.1186/s40562-015-0028-x

Geoscience Letters
a SpringerOpen Journal

RESEARCH LETTER
Open Access

# Evaluation of double-moment representation of ice hydrometeors in bulk microphysical parameterization: comparison between WRF numerical simulations and UND-Citation data during MC3E

Zhaoxia Pu* and Chao Lin

**Abstract**

The influence of double-moment representation of warm-rain and ice hydrometeors on the numerical simulations of a mesoscale convective system (MCS) over the US Southern Great Plains has been evaluated. The Weather Research and Forecasting (WRF) model is used to simulate the MCS with three different microphysical schemes, including the WRF single-moment 6-class (WSM6), WRF double-moment 6-class (WDM6), and Morrison double-moment (MORR) schemes. It is found that the double-moment schemes outperform the single-moment schemes in terms of the simulated structure, life cycle, cloud coverage, precipitation, and microphysical properties of the MCS. However, compared with UND-Citation observations, collected during the Midlatitude Continental Convective Clouds Experiment (MC3E), the WRF simulated ice hydrometeors with all three schemes do not agree well with the observations. Overall results from this study suggest that uncertainty in microphysical schemes could still be a productive area of future research from perspective of both model improvements and observations.

## Background

Microphysical parameterization (MP) is an important source of uncertainty in the numerical prediction of mesoscale convective systems (MCSs) (Randall et al. 2003). Due to the complexity of microphysical processes, various MP schemes have been developed based on different treatments of the number and size distributions of hydrometeor species. Many of these schemes are examples of the bulk MP scheme, which assumes that hydrometeor size distributions follow specific functional forms for either single-moment (1M hereafter) or multiple-moment representations (e.g., Milbrandt and Yau 2005a, b; Morrison et al. 2009). Specifically, a 1M scheme predicts only mixing ratio, whereas a double-moment scheme (2M hereafter) forecasts both mixing ratios and number concentrations of the hydrometeor size distributions for various hydrometeor species.

It has been recognized that different MP schemes can significantly influence the structure and evolution of an MCS in numerical simulations (e.g., Van Weverberg et al. 2013; Adams-Selin et al. 2013). Recent studies have suggested that numerical simulations with 2M of warm-rain and ice schemes can better simulate stratiform precipitation and convection-induced cold pool characteristics (e.g., Morrison et al. 2009; Van Weverberg and Vogelmann 2012). Other studies, however, have pointed out that using 2M for rain only can produce the same results as using a full 2M scheme (e.g., Morrison et al. 2009; Lim and Hong 2010). Since a major difference between the partial and full 2M schemes is the representation of ice species, and it is well known that the uncertainty in microphysics parameterizations arises mainly from the treatment of ice processes, the important question to ask is: are the full 2M treatments of ice hydrometeors

*Correspondence: Zhaoxia.Pu@utah.edu
Department of Atmospheric Sciences, University of Utah, 135 S, 1460 E, Rm. 819, Salt Lake City, UT 84112, USA

good enough in a current 2M scheme, such as the Morrison scheme that was included in the mesoscale community Weather Research and Forecasting (WRF) model (Skamarock et al. 2008)? Due to the lack of observations with detailed MCS cloud components, a detailed evaluation of 2M schemes has not yet been undertaken.

Fortunately, during April and May of 2011, the Midlatitude Continental Convective Clouds Experiment (MC3E) field program was conducted jointly by the U.S. Department of Energy and NASA in the Southern Great Plains in the central USA. With the overarching goal to provide the most complete characterization dataset for convective cloud systems, precipitation, and their environment as well as the representation of cumulus clouds in computer models that has never before been available, the campaign leveraged the largest observing infrastructure currently available with an extensive sounding array, remote sensing and in situ aircraft observations (Jensen et al. 2010). Among these data collected during the field campaign, the University of North Dakota Citation (UND-Citation) dataset provides measurements of hydrometeor distributions with hydrometeor properties, such as ice particle number concentration in specific diameter bins and ice water content inferred from the particle distributions. These data offer an excellent opportunity to evaluate the performance of microphysical schemes in predicting microphysical properties.

In this paper, we conduct the first study to compare the WRF model simulations with the UND-Citation dataset to obtain insight regarding the representation of ice hydrometeor properties in a 2M microphysical scheme. Section "A mesoscale convective case and WRF simulations" introduces the WRF model simulation of an MCS case. Section "Aircraft data" describes the UND-Citation data. Section "Comparison between WRF simulations and UND-Citation data" presents the comparison results, and a summary with concluding remarks is given in section "Summary and concluding remarks".

## A mesoscale convective case and WRF simulations

From NEXRAD observations, a convective system initiated at about 2100 UTC 23 May 2011 and moved out of the Oklahoma region at about 0600 UTC 24 May 2011. This convective system originally formed from isolated convective cells in western Oklahoma under the influence of the dry line and outflow boundary produced by the previous convective episode in northeastern Oklahoma. After the initiation, the convective system strengthened in both size and intensity in the next few hours and became a multicell mesoscale convective system (MCS) with a NE–SW orientation at 2300 UTC 23 May 2011. At 0000 UTC 24 May 2011, this MCS evolved into a mature stage with the cells organized in a S–N direction. The mature stage lasted about 3–4 h. Finally, this MCS began to dissipate at about 0400 UTC 24 May 2011 and slowly moved out of the Oklahoma region at about 0600 UTC 24 May 2011. The composite NEXRAD radar reflectivity in Figs. 1 and 2 reveals the convective evolution between 2145 UTC 23 May and 2345 UTC 23 May 2011, corresponding to the available aircraft data.

An advanced research version of the WRF model (Skamarock et al. 2008) version 3.4.1 is used for numerical simulation of the MCS. Three nested domains are used with horizontal grid sizes at 12, 4, and 1.33 km, respectively. Forty-six vertical sigma levels are employed. Initial and boundary conditions are derived from the NCEP North American Mesoscale (NAM) model analysis. Simulations cover the period from 0000 UTC 23 to 1200 UTC 24 May 2011. Physical parameterization schemes include: the Kain–Fritsch cumulus scheme (for the domain at 12 km grid size only; Kain 2004), the Rapid Radiative Transfer Model (RRTM; Mlawer et al. 1997) longwave and the Dudhia shortwave (Dudhia 1989) radiation schemes, the RUC (Rapid Update Cycle; Smirnova et al. 2000) land-surface scheme, and the Mellor–Yamada–Janjic (Janjic 1990) turbulent kinetic energy (TKE) PBL scheme. Three experiments with different MP schemes were conducted to examine the sensitivity of WRF simulations to different moment representations of warm-rain and ice hydrometeors in predicting MCS properties: the WRF single-moment 6-class (WSM6, 1M scheme, Hong and Lim 2006), WRF double-moment 6-class (WDM6, 2M representation of warm-rain only, Lim and Hong 2010), and Morrison double-moment (MORR, 2M representation of warm-rain and ice hydrometeors, Morrison et al. 2005) schemes.

The simulation results, as revealed by composite radar reflectivity, are shown in Fig. 1. To validate the model-simulated cloud properties, a radar reflectivity-based cloud classification algorithm is developed following the work of Steiner et al. (1995) and Feng et al. (2011). This algorithm classified the convective system into a convective core (CC), stratiform rain (SR), non-precipitating transitional anvil cloud (ACtrans), and anvil cloud (AC) from NEXRAD radar reflectivity observations (Fig. 2). Figures 1 and 2 suggests that the 2M representation of warm rain (WDM6) helps the model reproduce a better forecast of the MCS in terms of the cloud coverage and components, compared with the forecast from the experiment with a 1M scheme (WSM6). Moreover, further evaluations (see details in Lin 2014) indicated that: with a full 2M scheme (MORR), the model produces the best simulations with the proper convection life cycle and quantitative precipitation forecasting (QPF). Since the major difference between the MORR and WDM6 is the representation of ice species, the importance of including 2M representation of ice hydrometeors is evident. In the

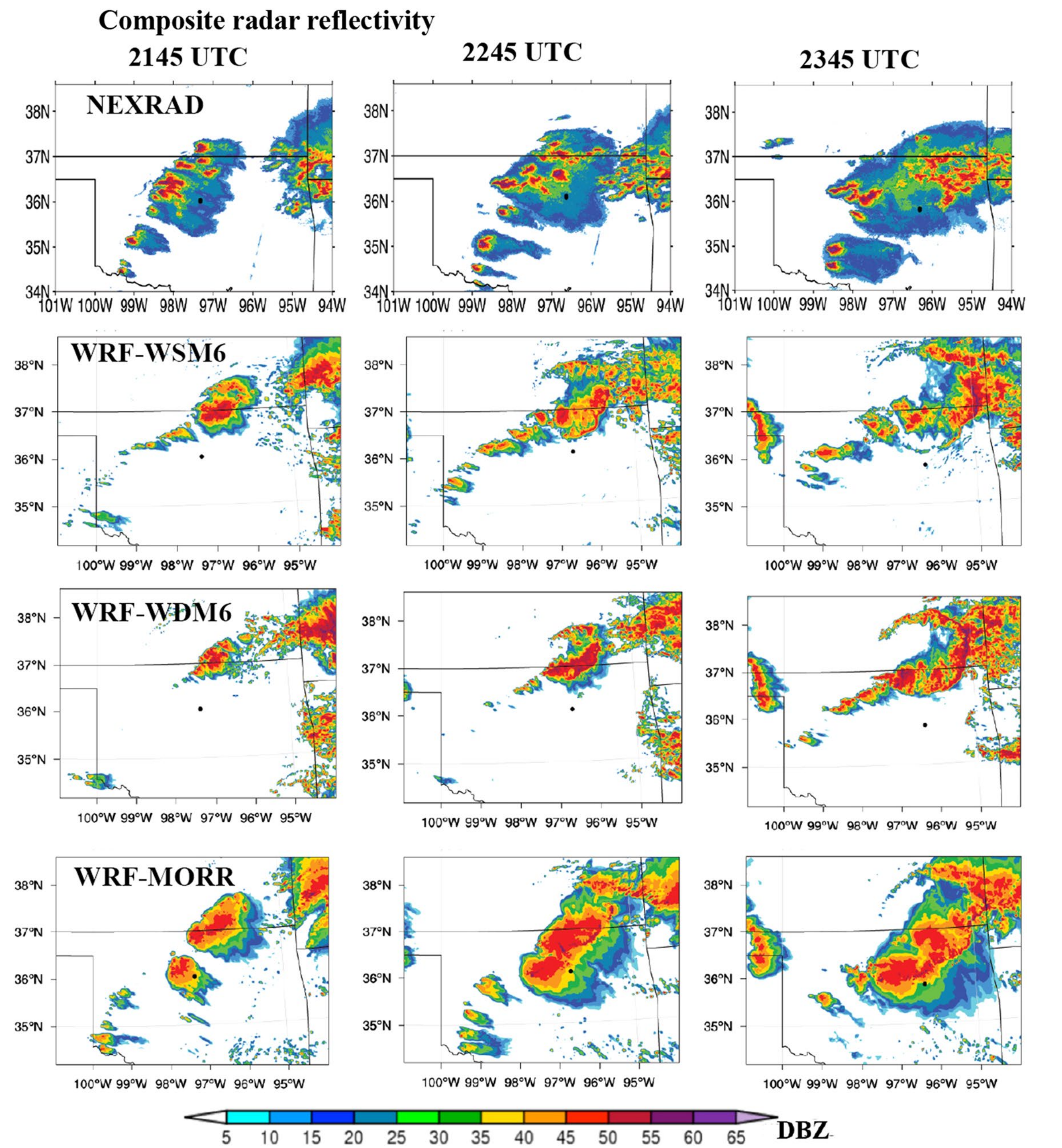


**Fig. 1** Composite radar reflectivity from NEXRAD observations (*top row*), WRF-WSM6 (*second row*), WRF-WDM6 (*third row*), and WRF-MORR (*bottom row*). From *left* to *right*, *columns* are at the time of 2145 UTC, 2245 UTC, and 2345 UTC 23 May 2011, respectively

following section, we compare the model simulation and aircraft observations of ice properties to confirm whether WRF simulation with MORR indeed improves the prediction of ice properties.

## Aircraft data

The UND aircraft operates at altitudes ranging from near the surface to 13 km. It is certified for its ability to fly into icing conditions (Delene 2011). Measurements from the UND-Citation have been used in many previous observational studies (e.g., Prenni et al. 2007; Sukovich et al. 2009). For the selected convection case in this study (23–24 May 2011), UND-Citation cloud microphysics data are available from 2100 UTC 23 to 0030 UTC 24 May 2011 at one-second intervals, which covers the developing and mature stages of the convection system. Considering

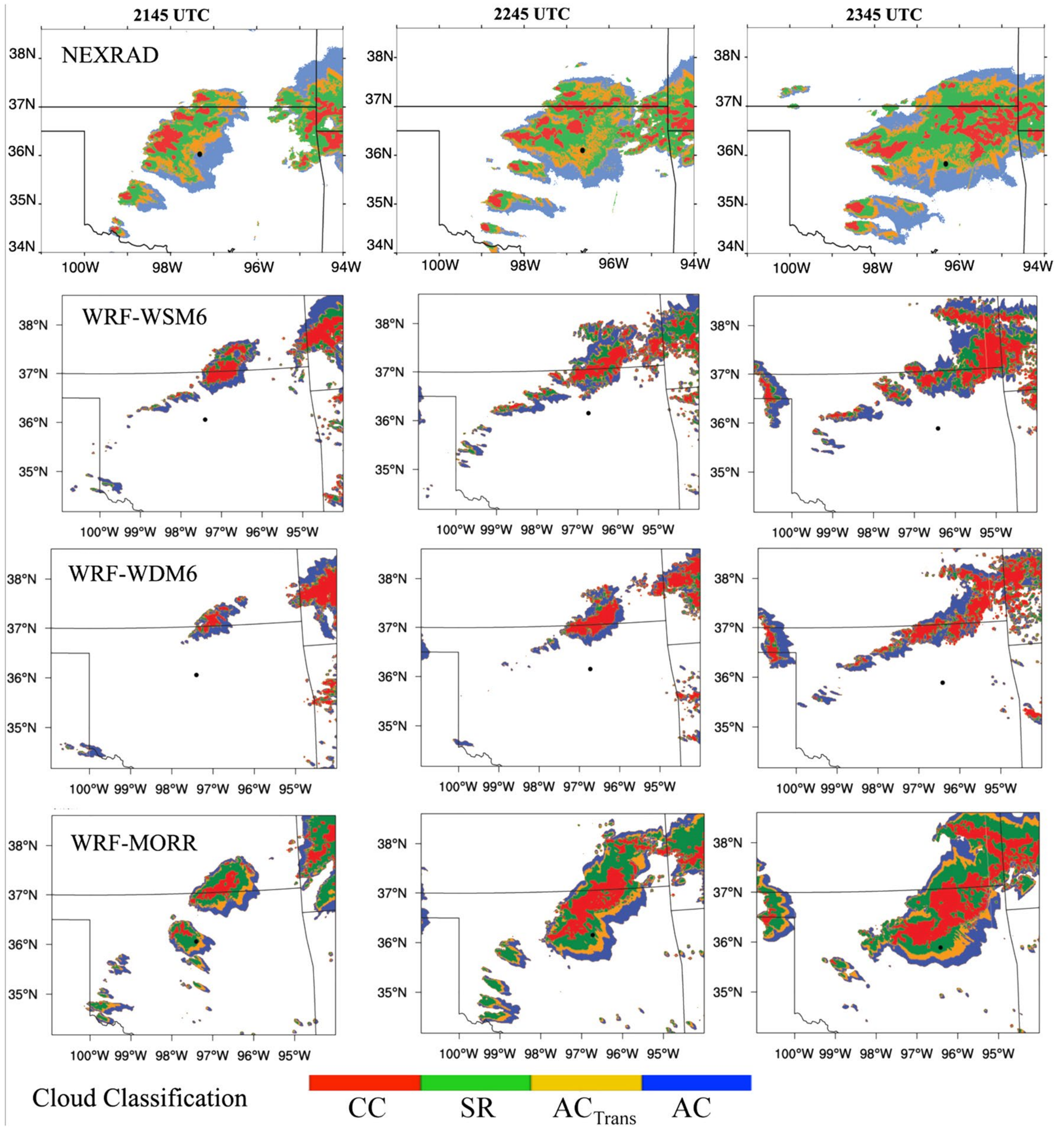


**Fig. 2** The same as Fig. 1, except for the cloud classification derived from the radar reflectivity, including convective core (*CC*), stratiform (*SR*) region, transitional anvil clouds (*ACtrans*), and anvil clouds (*AC*)

the variability and coverage of the convection system and the UND-Citation dataset, data between 2145 UTC 23 and 0015 UTC 24 May 2011 are used for the evaluations. The aircraft collected data at heights between 7 and 9 km during this period, mainly in the stratiform region of the convection system, where most of the composite NEXRAD radar reflectivity ranges from 20 to 30 dBZ.

The aircraft measures the ice water content (IWC) and number concentration using several instruments. Specifically, the number concentration (in each size bin) is measured by the particle measuring system (PMS) 2DC (33 to above 1000 μm), cloud particle imager (CPI), and high-volume particle spectrometer (HVPS) imaging probe, with ice particle sizes ranging from 200 μm to about 6 cm. The measurements contain records of flight time and aircraft latitude, longitude, and altitude. The IWC data come from two sources: one is the combined 2DC and HVPS number concentration dataset, with a resolution of about 2 μm and a minimum detectable size of about 20 μm, which provides detailed information on ice particle sizes ranging from 50 to 500 or 600 μm (Heymsfield et al. 2004). The IWC is calculated by Eq. (1).

$$\mathrm{IWC} = \sum_{D_{\min}}^{D_{\max}} N(D)M(D) \tag{1}$$

where $D_{\min}$ is the minimum diameter of the particles. $D_{\max}$ is the maximum diameter of the particles. $N(D)$ is the number of particles in the specific diameter bin, and $M(D)$ is the corresponding mass of the particle, calculated by $M(D) = 0.0061(D^{2.05})$ (Heymsfield et al. 2004). The other IWC data come from the Nevzorov probe. It provides a measurement of total water content (TWC) and liquid water content (LWC), which are fully calculated from first principles of heat transfer on the sensor wire (Korolev et al. 1998; Vidaurre et al. 2011). The IWC is the difference between the TWC and LWC.

## Comparison between WRF simulations and UND-Citation data

The aircraft track is located mostly between 7 and 9 km in height, ranging from the 29th to 32nd model levels. Since the space between the model levels is sparse (~1 km), to avoid the uncertainty introduced by the vertical interpolation, we compare the UND-Citation data with the model values at the nearest model vertical level. Meanwhile, compared with NEXRAD observations, the WRF simulations of the convection system have both position and coverage errors (Figs. 1, 2). Therefore, it is difficult to directly compare the UND-Citation observations with the simulations. Thus, a method of comparison is designed based on the classification of the convective system using 3D distribution of radar reflectivity. The details of the comparison procedure are as follows:

(1) Classify the convection system into different components, namely, convection core (CC), stratiform rain (SR) region, transitional anvil ($AC_{Tran}$) region, and anvil (AC) region for both the NEXRAD observations and the WRF simulations based on the 3D radar reflectivity distribution, following the method in Feng et al. (2011). Figure 2 shows samples of the classification results. (2) Average the microphysical properties (e.g., ice mixing ratio, IWC, and ice particle number concentration) produced by the simulations over space for each cloud component. (3) Average the UND-Citation data over 5-min time intervals to: (a) be able to obtain enough samples to

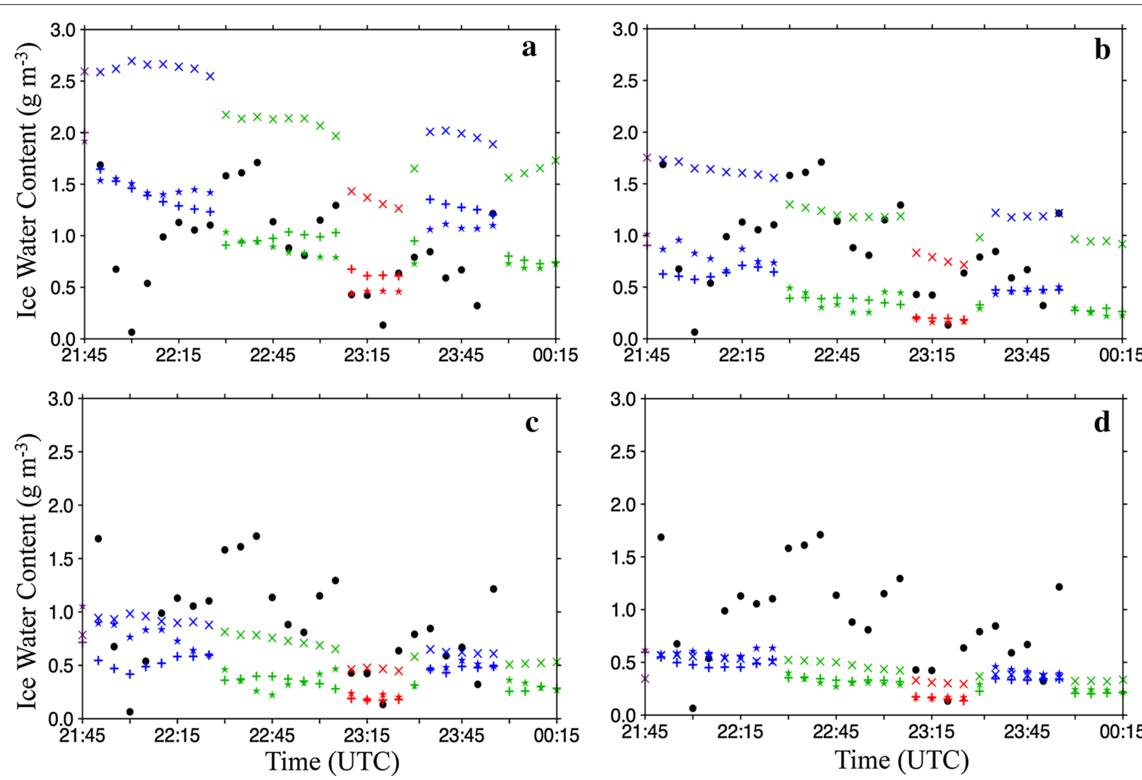


**Fig. 3** Time series of the averaged (**a**–**d**) ice water content from observations (*black dots*) and simulations over various convective components (**a** over CC region, **b** over SR region, **c** over ACtrans region and **d** over AC region) from different experiments: WRF-WSM6 ("+"), WRF-WSM6 ("*"), WRF-MORR ("x") at the nearest model levels: *purple*: 29th level; *blue*: 30th level; *green*: 31st level; and *red*: 32nd level

calculate the average and (b) accommodate the 5-min data intervals in the WRF simulations. (4) Compare the area-averaged values of the WRF simulations for each convection component with the temporal average values of the UND-Citation data at the same valid times.

Fortunately, large enough samples (about several thousands) are available in each case to achieve the comparison.

### Ice water content (IWC)

We first select the IWC inferred from combined 2DC and HVPS probes for the comparison. Because the IWC in the dataset is derived from large particles only (those with diameters larger than 100 μm), to be consistent with the data, only the IWC values of snow and graupel in model simulations are counted to compare with aircraft observations. Figure 3a, b, c, and d compare the averaged IWC over different convection components

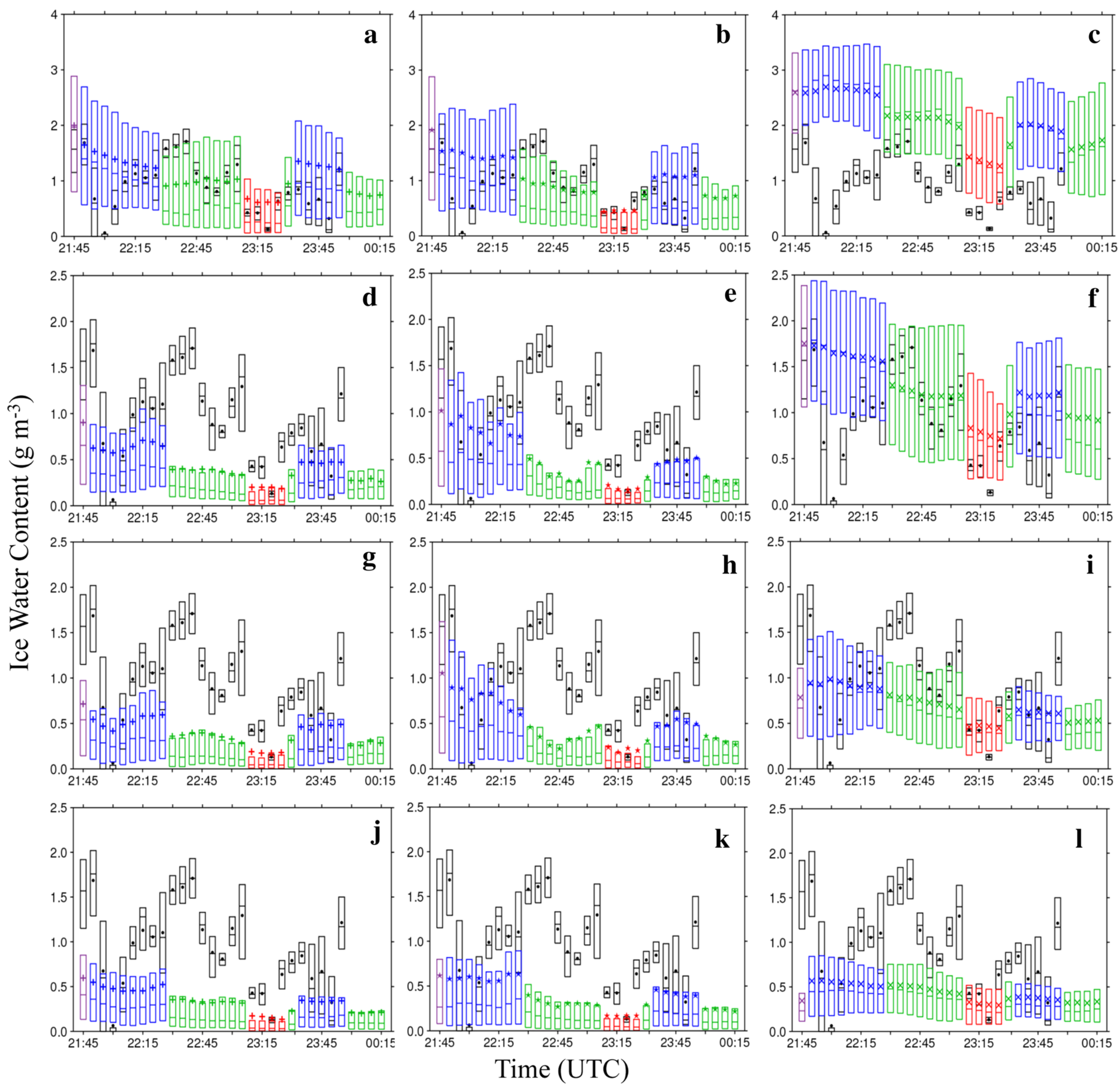


**Fig. 4** Probability distribution with percentiles of 75 % (*upper limit*), 50 % (median), and 25 % (*bottom limit*) for the ice water content from observations (*black*) and simulations (*left panels* WRF-WSM6; *middle panels* WRF-WDM6; and *right panels* WRF-MORR). From *top* to *bottom*, the values are averaged over different convection components [CC: (**a**–**c**), SR: (**d**–**f**), ACtrans: (**g**–**i**), and AC: (**j**–**l**)]. *Colors* the comparison at nearest model levels: purple: 29th level; *blue*: 30th level; *green*: 31st level; and *red*: 32nd level

between simulations and aircraft observations. Relatively large variability is found in the time series of the IWC. The IWC shows a decreasing trend from the CC (Fig. 3a) to the AC region (Fig. 3d). WRF-MORR produces a larger IWC than WRF-WSM6 and WRF-WDM6 do. For the SR region (Fig. 3b), WRF-MORR produces a realistic IWC, while WRF-WSM6 and WRF-WDM6 underestimate the IWC. The IWC values derived from the simulations in the ACtrans (Fig. 3c) and AC (Fig. 3d) regions are very smooth and are smaller than the observations, which may be caused by the small amount of graupel in the ACtrans region, because graupel dominates the ice water content.

To eliminate the uncertainty due to averaging over space (simulations) and time (UND-Citation data), the spatial and temporal probability distributions with percentiles of 75 and 25 % of IWC for different convection components are shown in Fig. 4. Large discrepancies are found between observations and simulations in the SR region (Fig. 4d–f), ACtrans region (Fig. 4g–i) and AC region (Fig. 4j–l). WRF-WSM6 (Fig. 4d) and WRF-WDM6 (Fig. 4e) underestimate IWC, while WRF-MORR (Fig. 4f) produces a relatively realistic IWC. Similar conclusions are found for the IWC in the ACtrans region. Overall, among all numerical simulations, WRF-MORR produces relatively comparable IWC with observations. However, as mentioned above, during MC3E, there are two data sources for the IWC. One is the 2DC and HVPS probes; the other is the Nevzorov probe. When IWC from these two data sources are compacted, it is found that the 2DC and HVPS produce much higher IWC than the Nevzorov probe (Fig. 5). Note that the above IWC comparisons were done with the values derived from the 2DC and HVPS probes. If the simulations were compared with the data collected from the Nevzorov probe, WRF-WSM6 and WRF-WDM6 would match the observations better than WRF-MORR. The difference, arising from the two IWC datasets, illustrates the significant influence of the observation uncertainties.

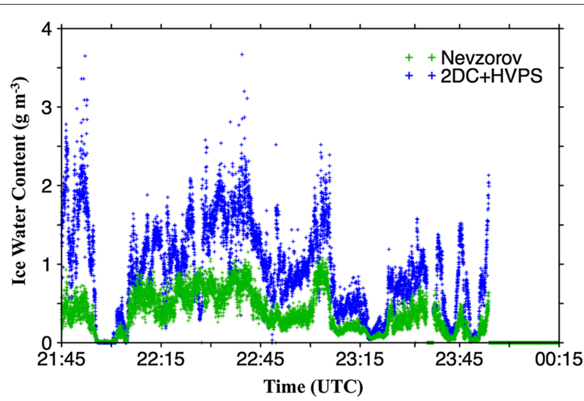

**Fig. 5** Time series of ice water content observed by 2DC and HVPS probes (*blue dots*) and by Nevzorov probe (*green dots*). The time interval is one second for both datasets

### Number concentration

The number concentration collected by the UND-Citation aircraft is measured by the 2DC and HVPS probes for particles with diameters larger than 100 μm. In the model simulations, considering the small size of ice phase hydrometeors, only the number concentrations of snow and graupel are considered. Among the three MP schemes used in this study, the MORR scheme treats the snow and graupel hydrometeors as 2M species, as WRF-MORR predicts the mixing ratio and number concentration of graupel and snow. However, the WSM6 and WDM6 schemes treat snow and graupel as 1M species; thus, the number concentration is diagnosed from the mixing ratio and other parameters. Specifically, the particle size distribution of snow and graupel used in WSM6 and WDM6 are treated as a gamma function. The number concentration for the specific diameter range is calculated by the integral of the particle size distribution (Lim and Hong 2010).

To compare the number concentrations between the model simulations and observations, the spatial and temporal probability distributions with percentiles of 75 and 25 % of the number concentration of the model simulations, and the observations, are shown in Fig. 6. The UND-Citation shows a very large variability in number concentration, but the average values from the simulations show a steady trend. The simulated number concentration does not capture the observed large frequency variability in the ice particle number concentration in all three WRF forecasts with WSM6, WDM6 and MORR.

## Summary and concluding remarks

In this study, the WRF-simulated microphysical properties of ice water content and total ice particle number concentration are validated using the UND-Citation aircraft observations in the developing and mature stages of a mesoscale convective system. The results suggest that 2M representations of ice hydrometeors in Morrison MP scheme help the WRF model to reproduce a better forecast of MCS but does not seem to produce the realistic ice properties. While the simulation with MORR may produce reasonable IWC when compared with the 2DC and HVPS data, there are clear uncertainties in the IWC datasets since large discrepancies are found in IWC measurements from the Nevzorov probe and 2DC and HVPS probes. The total ice number

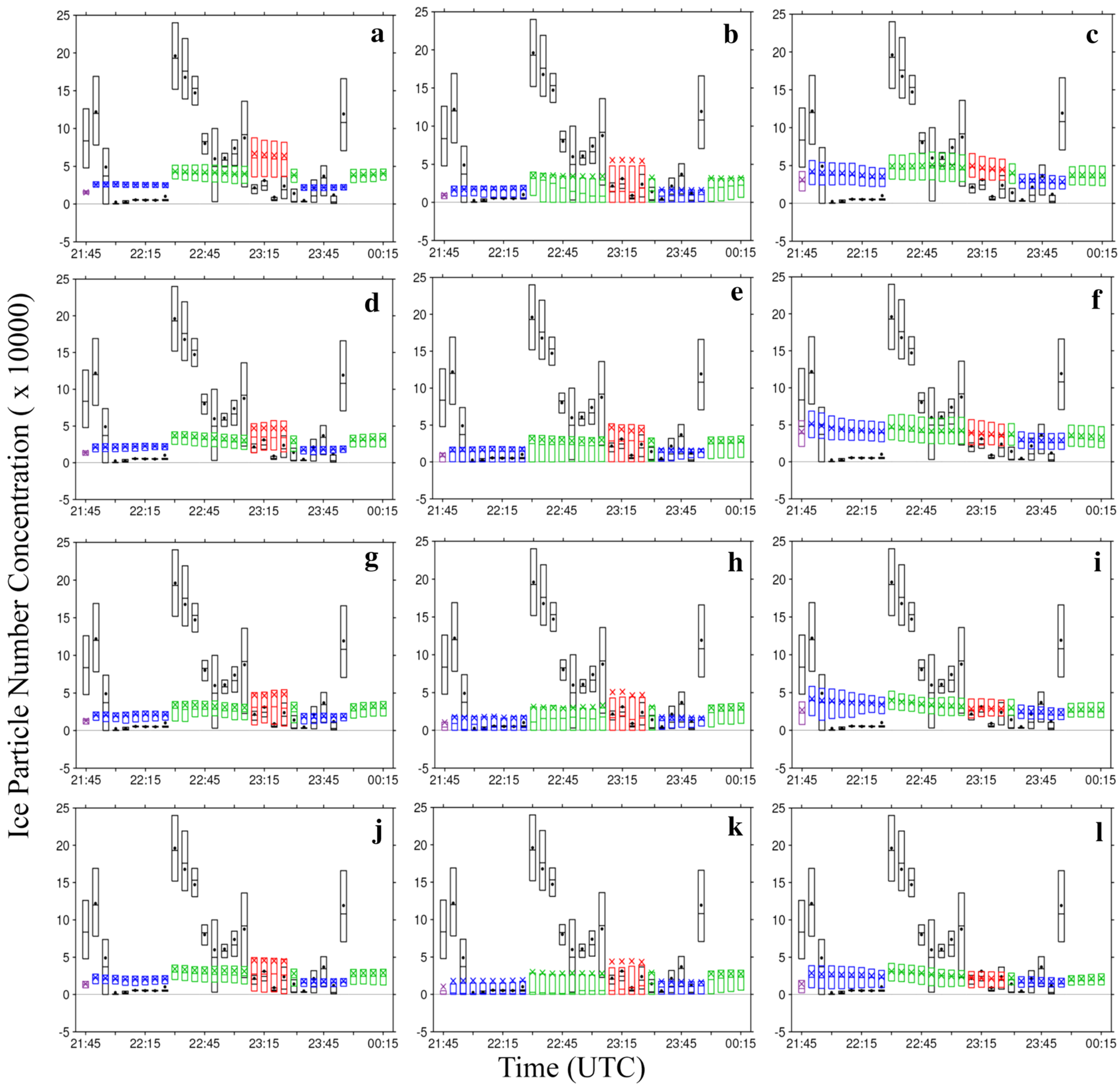


**Fig. 6** Same as Fig. 4, except for the number concentration of ice phase particles with diameters larger than 100 μm

concentrations produced by the model are different from the observations.

Overall, the WRF-simulated ice hydrometeors with all three schemes do not agree well with the observations. The reasons of the disagreements may be, but are not limited to, the following: (1) the model did not reproduce convection structures exactly. (2) The errors in the aircraft measurements play an important role. (3) The aircraft data are too sparse to compare with the model, as the aircraft sampled only one point at each specific time. More accurate and dense observations are needed to make a more effective comparison. Nevertheless, results from this study suggest that the uncertainty in microphysical schemes could be a productive area of future research from perspective of both model improvements and observations.

**Authors' contributions**

Dr. ZP originated the research, guided the whole study and also finalized the manuscript. CL conducted computing work, initiated the summary of results. Both authors read and approved the final manuscript.

**Acknowledgements**

Authors appreciate valuable comments from Drs. Steven Krueger and Jay Mace at the University of Utah. This study is supported by the Office of Science (BER), US Department of Energy Grant No. DE-SC0007060 through

Atmospheric System Research Program. Dr. ZP is also supported by NASA Water and Energy Cycle Study Program through Award NNX15AD14G. The authors would like to thank the DOE/NASA MC3E team, University of North Dakota and NCAR for obtaining and processing UND-Citation observations. The WRF model and associated documents are free available for downloading at http://www.wrf-model.org with a web registration.

### Competing interests
The authors declare that they have no competing interests (both financial and non-financial ones).

Received: 12 July 2015 Accepted: 20 October 2015
Published online: 04 November 2015

### References
Adams-Selin RD, ven den Heever SC, Johnson RH. Impact of graupel parameterization schemes on idealized bow echo simulations. Mon Weather Rev. 2013;141:1241–62.
Delene DJ. Airborne data processing and analysis software package. Earth Sci Inform. 2011;4:29–44.
Dudhia J. Numerical study of convection observed during the winter monsoon experiment using a mesoscale two-dimensional model. J Atmos Sci. 1989;46:3077–107.
Feng Z, Dong X, Xi B, Schumacher C, Minnis P, and Khaiyer M. Top-of-atmosphere radiation budget of convective core/stratiform rain and anvil clouds from deep convective systems. J Geophys Res. 2011;116. doi:10.1029/2011JD016451.
Heymsfield AJ, Bansemer A, Schmitt C, Twohy C, Poellot MR. Effective ice particle densities derived from aircraft data. J Atmos Sci. 2004;61:982–1003.
Hong SY, Lim JO. The WRF single-moment 6-class microphysics scheme (WSM6). J Korean Meteor Soc. 2006;42:129–51.
Janjic ZI. The step-mountain coordinate: physical package. Mon Weather Rev. 1990;118:1429–43.
Jensen MP, Hou AY, Petersen WA, Kollias P, Del Genio AD, Orr B, Rutledge SA, Schwaller MR, Zipser E. Midlatitude continental convective clouds experiment (MC3E) science plan. US Department of Energy Doc. DOE/SC-ARM/10-004, p. 31; 2010.
Kain JS. The Kain–Fritsch convective parameterization: an update. J Appl Meteor. 2004;43:170–81.
Korolev AV, Strapp JW, Isaac GA, Nevzorov AN. The Nevzorov airborne hot-wire LWC-TWC probe: principle of operation and performance characteristics. J Atmos Ocean Tech. 1998;15:1495–510.
Lim KS, Hong SY. Development of an effective double-moment cloud microphysics scheme with prognostic cloud condensation nuclei (CCN) for weather and climate models. Mon Weather Rev. 2010;138:1587–612.
Lin C. Evaluation of double-moment representation of warm-rain and Ice hydrometeors in bulk microphysical parameterization. M.S. Thesis, University of Utah, p. 111; 2014. **(Available at request: Department of Atmospheric Sciences, University of Utah, 135 S 1460 E, Rm. 819, Salt Lake City, UT 84112, USA).**
Milbrandt JA, Yau MK. A multimoment bulk microphysics parameterization. Part I: analysis of the role of the spectral shape parameter. J Atmos Sci. 2005a;62:3051–64.
Milbrandt JA, Yau MK. A multimoment bulk microphysics parameterization. Part II: a proposed three-moment closure and scheme description. J Atmos Sci. 2005b;62:3065–81.
Mlawer EJ, Taubman SJ, Brown PD, Iacono MJ, Clough SA. Radiative transfer for inhomogeneous atmospheres: RRTM, a validated correlated k model for the longwave. J Geophys Res Atmos. 1997;102:16663–82.
Morrison H, Thompson G, Tatarskii V. Impact of cloud microphysics on the development of trailing stratiform precipitation in a simulated squall line: comparison of one- and two-moment schemes. Mon Weather Rev. 2009;137:991–1007.
Morrison H, Curry JA, Khvorostyanov VI. A new double-moment microphysics parameterization for application in cloud and climate models. Part I: description. J Atmos Sci. 2005;62:1665–77.
Prenni AJ, DeMott PJ, Kreidenweis SM, Harrington JY, Avramov AV, Olsson PQ. Can ice-nucleating aerosols affect arctic seasonal climate? Bull Am Meteor Soc. 2007;88:541–50.
Randall DA, Khairoutdinov MF, Arakawa A, Grabowski WW. Breaking the cloud parameterization deadlock. Bull Amer Meteor Soc. 2003;84:1547–64.
Skamarock WC, Klemp JB, Dudhia J, Gill DO, Barker DM, Duda MG, Huang XY, Wang W, Powers JG. A description of the advanced research WRF version 3. NCAR Tech Note NCAR/TN-475 + STR (p. 113); 2008.
Smirnova TG, Brown JM, Benjamin SG, Kim D. Parameterization of cold-season processes in the MAPS land-surface scheme. J Geophys Res. 2000;105:4077–86.
Steiner M, Houze RA Jr, Yuter SE. Climatological characterization of three-dimensional storm structure from operational radar and rain gauge data. J Appl Meteor. 1995;34:1978–2007.
Sukovich EM, Kingsmill DE, Yuter SE. Variability of graupel and snow observed in tropical oceanic convection by aircraft during TRMM KWAJEX. J Appl Meteor Climatol. 2009;48:185–98.
Vidaurre G, Hallett J, Rogers DC. Airborne measurement of liquid and total water content. J Atmos Ocean Tech. 2011;28:1088–103.
Van Weverberg K, Vogelmann AM. Sensitivity of idealized squall-line simulation to the level of complexity used in two-moment bulk microphysics schemes. Mon Weather Rev. 2012;140:1883–907.
Van Weverberg K, Vogelmann AM, Lin W, Luke EP, Cialella A, Minnis P, Khaiyer M, Boer, ER and Jensen MP. The role of cloud microphysics parameterization in the simulation of mesoscale convective system clouds and precipitation in the Tropical Western Pacific. J Atmos Sci. 2013;70:1104–28.